Supplemental Figure 1.

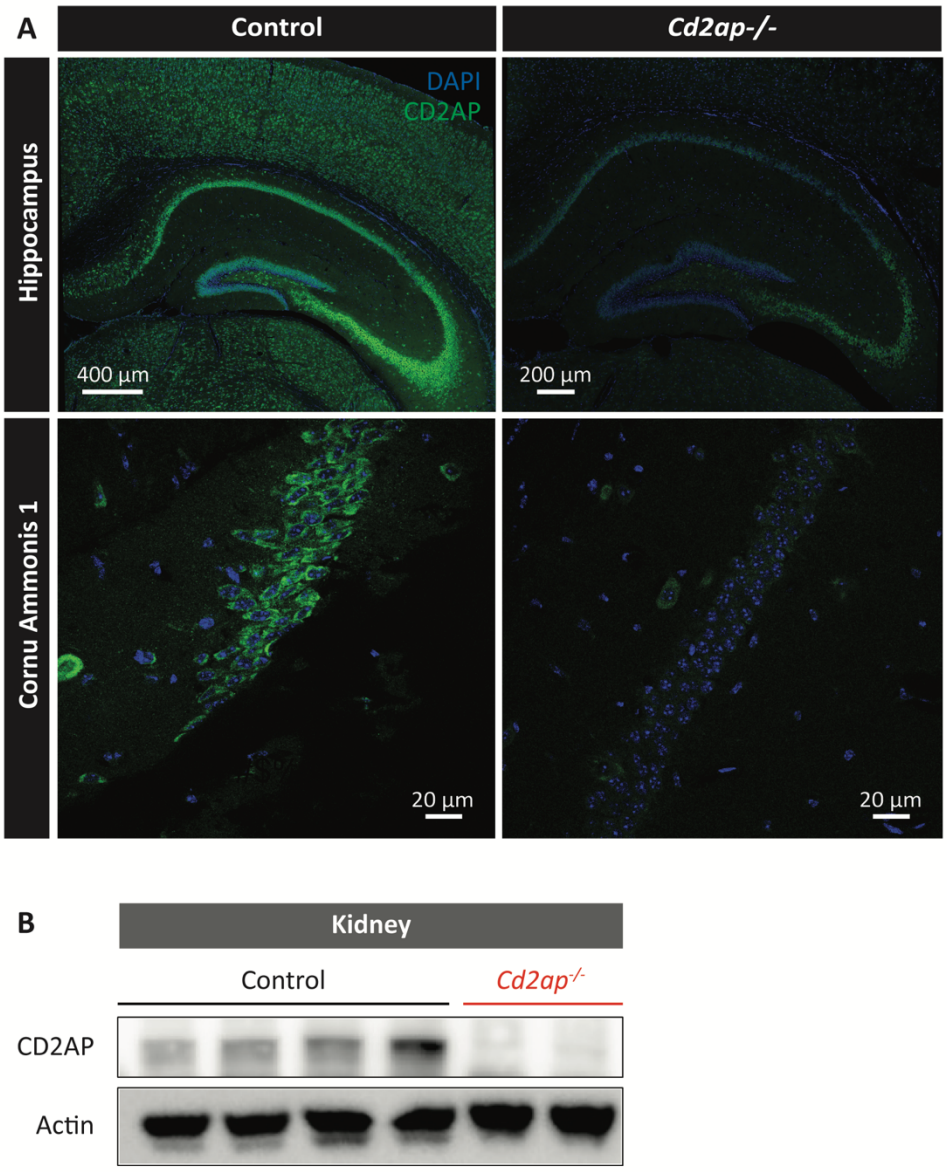

Supplemental Figure 1. Specificity of anti-CD2AP antibody for tissue staining and Western blotting.

(A) Brain slices from 5-week-old wildtype control and homozygous *Cd2ap*$^{-/-}$ germline knockout animals were stained using novel primary CD2AP antibody (1:2,000).

(B) Western blotting of mouse kidney homogenates using the anti-CD2AP antibody (1:200) reveals a specific 80kDa band.

Supplemental Figure 2.

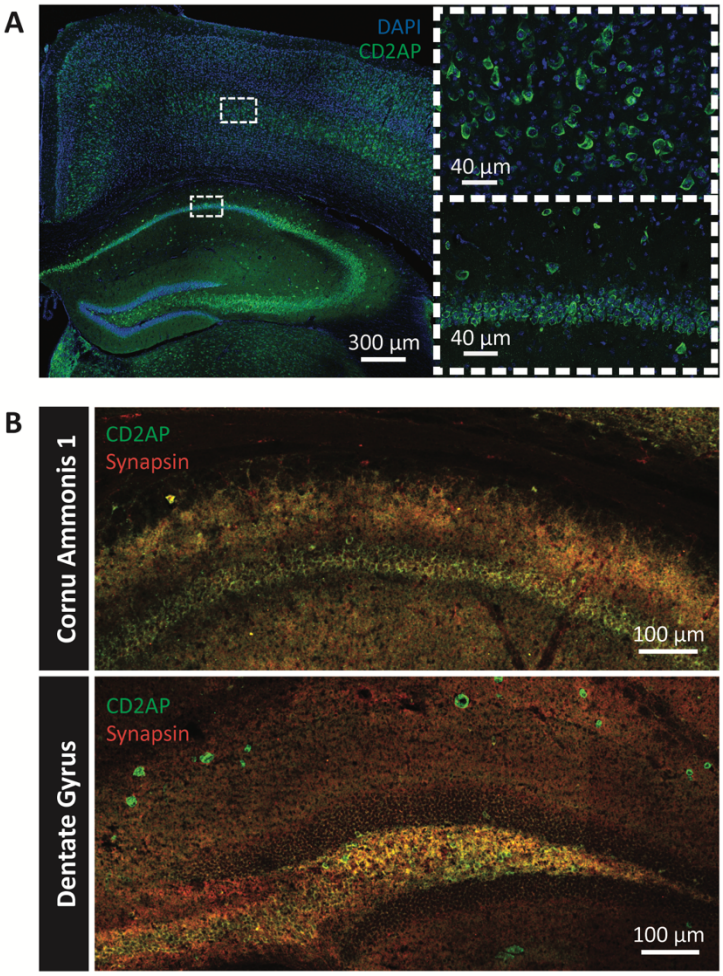

Supplemental Figure 2. Additional studies of *Cd2ap* expression in the mouse brain.

(A) CD2AP (green) is detected in the cortex (inset, top right) and the hippocampal CA1 region (inset, bottom right), as well as in the CA2, CA3, and the dentate gyrus (DG) hilus and polymorphic layer. Nuclei are counterstained with DAPI (blue).

(B) CD2AP (green) shows overlapping localization with the pre-synaptic marker Synapsin (red) in the mouse hippocampus CA1 and dentate gyrus.

Supplemental Figure 3.

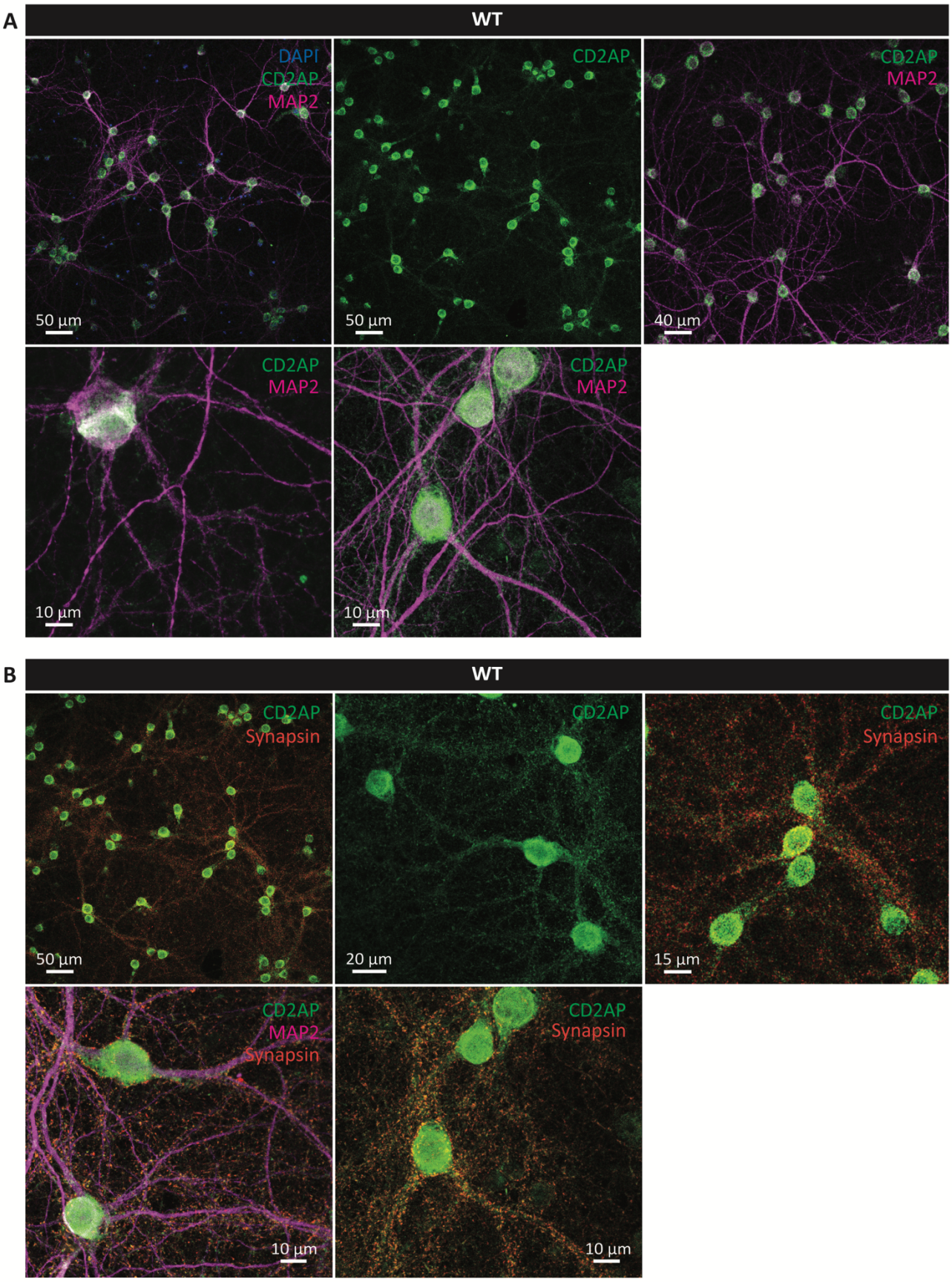

Supplemental Figure 3. Additional CD2AP staining localization in cultured neurons.
(A) CD2AP (green) staining overlaps with the neuronal marker MAP2 (magenta).
(B) CD2AP (green) staining also overlaps with Synapsin (red).
All images are of cultured wildtype (WT) DIV14 mouse cortical neurons.

Supplemental Figure 4.

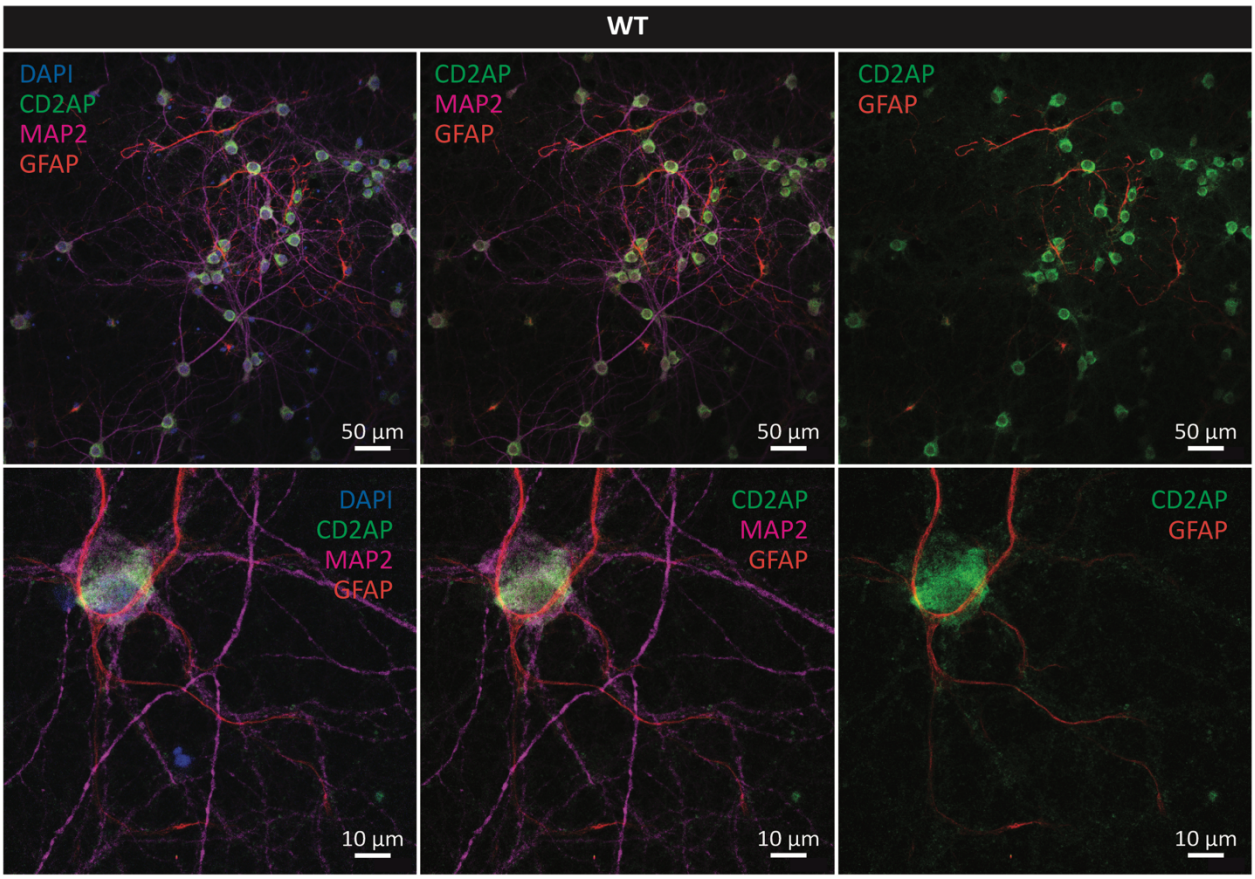

Supplemental Figure 4. CD2AP appears poorly expressed in mouse astrocytes.

CD2AP (green) has minimal overlap with the astrocyte marker, GFAP (red). Nuclei (DAPI, blue) and MAP2 (magenta) were also co-stained. All images are of wildtype (WT) cultured DIV14 mouse cortical neurons.

Supplemental Figure 5.

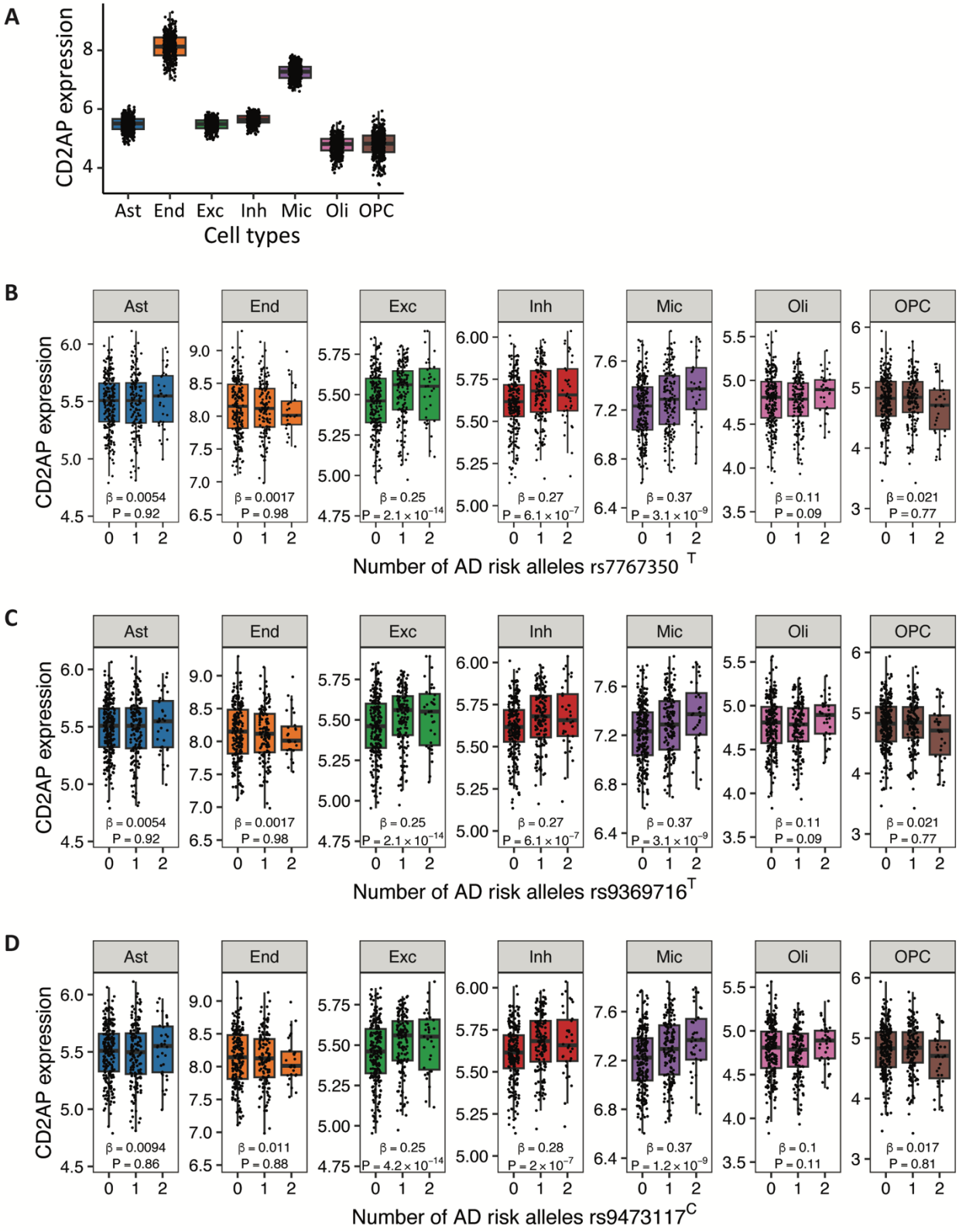

Supplemental Figure 5. Single-nucleus expression quantitative trait loci (eQTL) analysis.

(**A**) Cell type-specific expression of *CD2AP* is shown for astrocytes (Ast), endothelial cells (End), excitatory (Exc) and inhibitory (Inh) neurons, microglia (Mic), oligodendrocytes (Oli), and oligodendrocyte progenitor cells (OPC) in a dataset from human dorsolateral prefrontal cortex (N=424 samples). Box plots show risk variants *rs7767350* **(B)**, *rs9369716* **(C)**, and *rs9473117* **(D)** are associated with increased *CD2AP* expression in excitatory and inhibitory neurons and microglia. The frequency (odds ratio) for each of the SNPs considered here is as follows, based on the GWAS publications: rs9473117, 0.28 (1.09); rs7767350, 0.27 (1.08); and rs9369716, 0.27 (OR not reported, but consistent direction of effect based on regression coefficient).

Supplemental Figure 6.

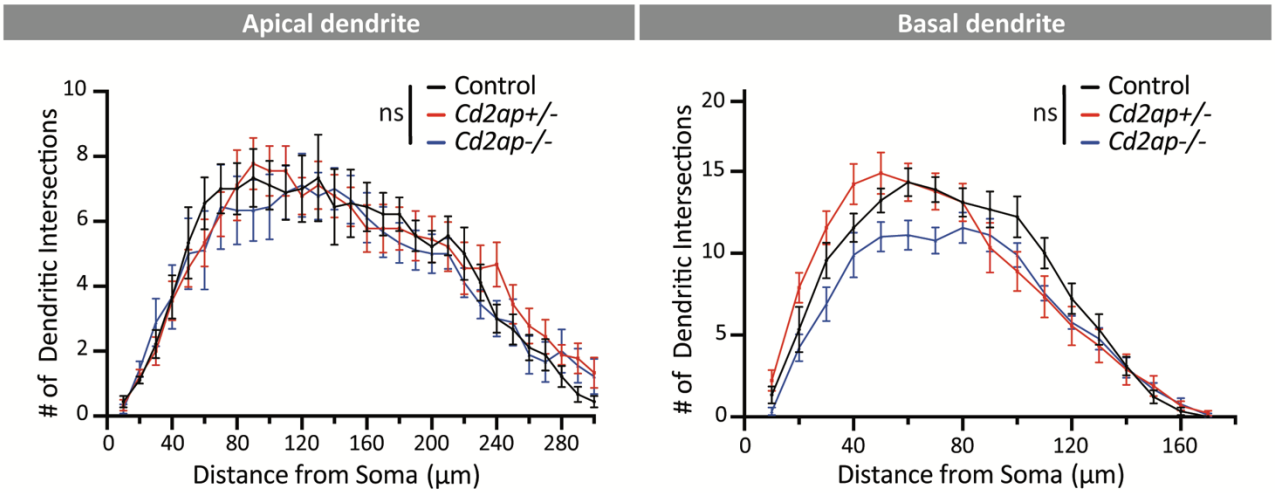

Supplemental Figure 6. Sholl analysis of hippocampal neurons in *Cd2ap* mice.

In hippocampal CA1 pyramidal neurons from 5-6-weeks-old mice, neither *Cd2ap* homozygous or heterozygous animals show any significant change in the number of dendritic Sholl intersections, including among either apical or basal dendrites. Statistical analysis was performed using linear mixed-effects models, with Tukey's post-hoc test, and sample sizes of N = 9 cells for each group (2F and 7M control cells; 6F and 3M *Cd2ap*$^{+/-}$ cells; 9M *Cd2ap*$^{-/-}$ cells), from at least 2 independent animals per genotype. All error bars denote mean ± SEM.

Supplemental Figure 7.

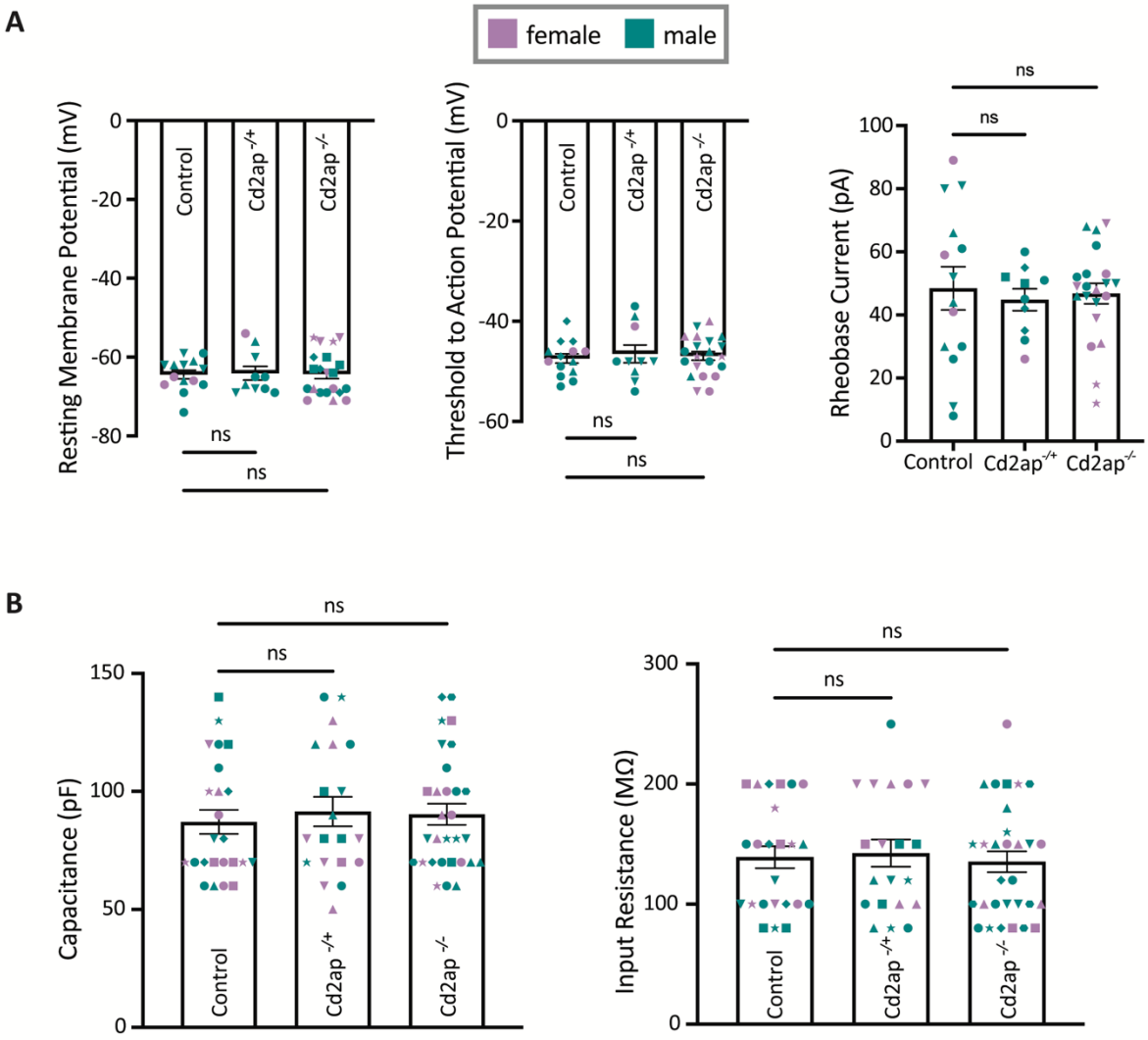

Supplemental Figure 7. Basal membrane neurophysiology in *Cd2ap* hippocampus.

(A) Neither *Cd2ap* homozygous nor heterozygous animals show significant differences in intrinsic biophysical properties of hippocampal neurons, including resting membrane potential, threshold to action potential, or rheobase current ($P > 0.05$). Statistical analysis was based on one-way ANOVA with Dunnett's post-hoc test, and sample sizes (N cells recorded): WT = 14 (3 female and 11 male); *Cd2ap*$^{+/-}$ = 10 (1F and 9M); and *Cd2ap*$^{-/-}$ = 21 (10F and 11M). Sample sizes (N mice) were as follows: WT = 4 (1F and 3M); *Cd2ap*$^{+/-}$ = 4 (1F and 3M); *Cd2ap*$^{-/-}$ = 7 (4F and 3M). Recordings were performed from at least 4 independent animals per genotype. All error bars denote mean ± SEM.
(B) Neither *Cd2ap* homozygous nor heterozygous animals show any significant differences in membrane capacitance or input resistance of hippocampal neurons ($P > 0.05$). Statistical analysis was performed using one-way ANOVA with Dunnett's post-hoc test, with sample sizes (N slices recorded): WT = 24 (11F and 13M); *Cd2ap*$^{+/-}$ = 20 (9F and 11M); and *Cd2ap*$^{-/-}$ = 30 (10F and 20M). Sample sizes (N mice) were as follows: WT = 11 (5F and 6M); *Cd2ap*$^{+/-}$ = 9 (4F and 5M); *Cd2ap*$^{-/-}$ = 11 (4F and 7M). Recordings were performed from at least 9 independent animals per genotype. All error bars denote mean ± SEM.

For all three genotypes, datapoints (cells) from different animals within a gender are represented by different shapes. Cells that originated from male mice are teal and cells that originated from female mice are lavender.

Supplemental Figure 8.

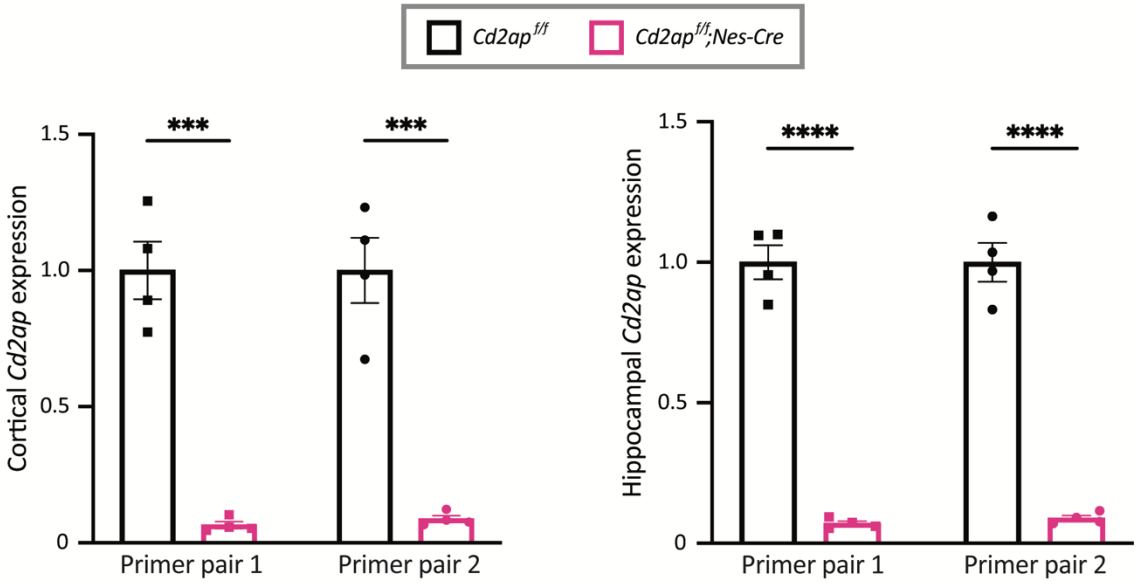

Supplemental Figure 8. Validation of *Cd2ap* conditional knockout mouse.

Four-month-old *Cd2ap* conditional knockout mice (*Cd2ap*$^{f/f}$*;Nes-Cre*) show decreased expression of *Cd2ap* mRNA compared to control *Cd2ap*$^{f/f}$ mice in the cortex (left) and the hippocampus (right), based on quantitative PCR. Statistical analysis was performed using t-tests, with sample sizes of N = 4 for each genotype. ***, $P < 0.001$; ****, $P < 0.0001$. All error bars denote mean ± SEM.

Supplemental Figure 9.

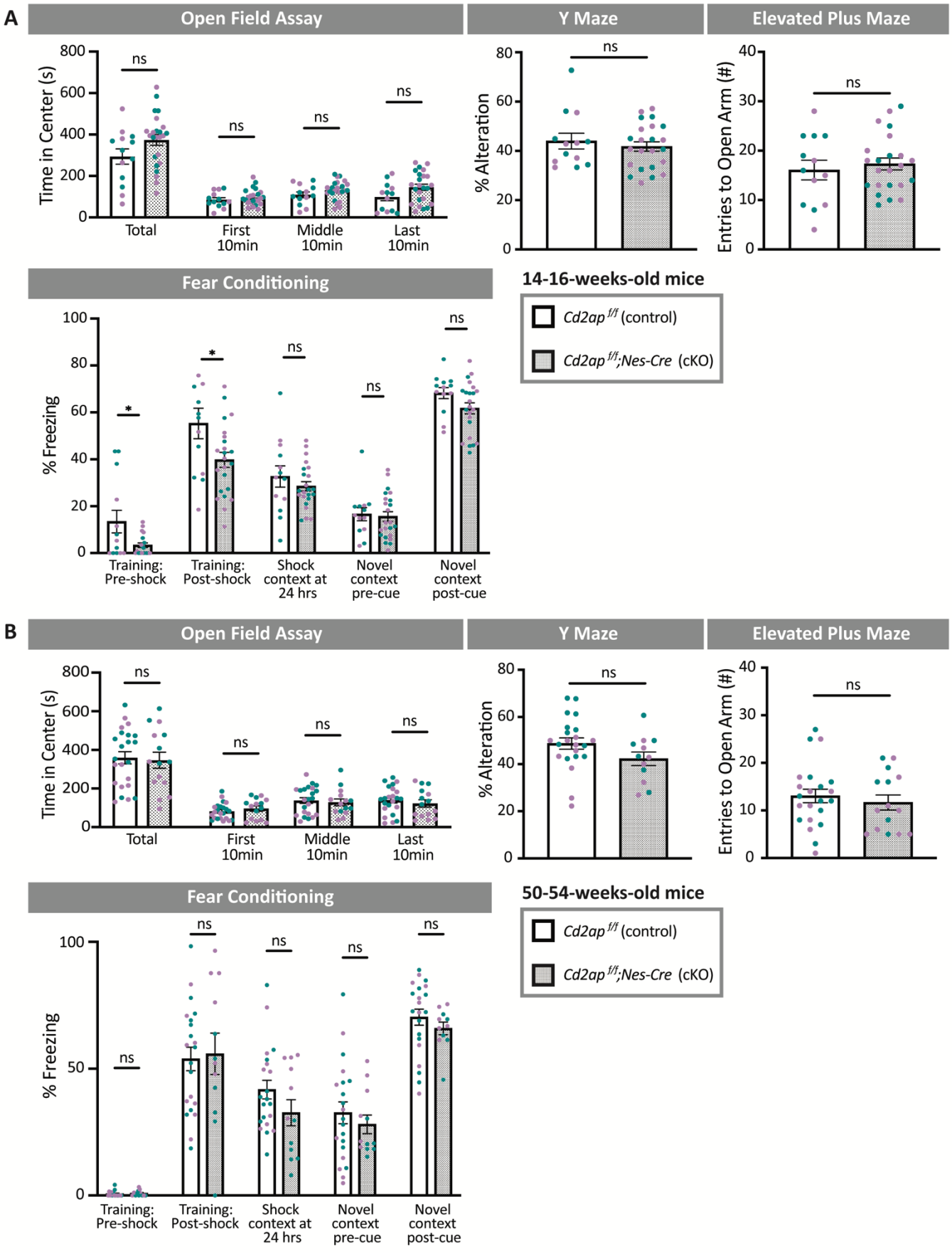

Supplemental Figure 9. Additional behavioral analysis of *Cd2ap* conditional knockout mice.

Results are shown following additional behavioral tests of *Cd2ap* conditional knockout animals (cKO; *Cd2ap$^{f/f}$;Nes-Cre*) and controls (*CD2AP$^{f/f}$*). Mice were examined at either 3.5- **(A)** or 12-months of age **(B)**. Overall, no significant differences were detected (all $P > 0.05$), except for decreased freezing among 3.5-month-old *Cd2ap* conditional knockout mice during the fear conditioning assay training ("pre-" and "post-shock"). Statistical analysis was performed using t-tests. For tests of young mice, samples sizes of N = 24 cKO (with 14F and 10M) and 13 control (with 6F and 7M) mice were used for the open field assay, N = 23 cKO (with 13F and 10M) and 13 control (with 6F and 7M) mice for fear conditioning, and N = 23 cKO (with 13F and 10M) and 13 control (with 6F and 7M) mice for Y-maze and elevated plus maze. In the fear conditioning training ("pre-shock"), three datapoints were identified as outliers and excluded, resulting in final N = 20 cKO (with 12F and 8M). For studies of aged mice, sample sizes were of N = 15 cKO (with 9F and 6M) and 23 (with 11F and 12M) control mice were used for the open field assay, N = 12 cKO (with 6F and 6M) and 22 (with 10F and 12M) control mice for Y-maze, N = 15 cKO (with 9F and 6M) and 22 (with 10F and 12M) control mice for elevated plus maze, and N = 12 cKO (with 6F and 6M) and 21 (with 9F and 12M) control mice for fear conditioning. In the fear conditioning training ("pre-shock"), five datapoints were identified as outliers and excluded, resulting in final N = 16 controls (8F and 8M). Also, for fear conditioning "novel context" (post-cue), one outlier datapoint was excluded, resulting in final N = 11 cKO (6F and 5M) for that test. The color of individual data points indicates the sex of each animal, with teal indicating male mice and lavender indicating female mice. *, $P < 0.05$. All error bars indicate mean ± SEM.

Supplemental Figure 10.

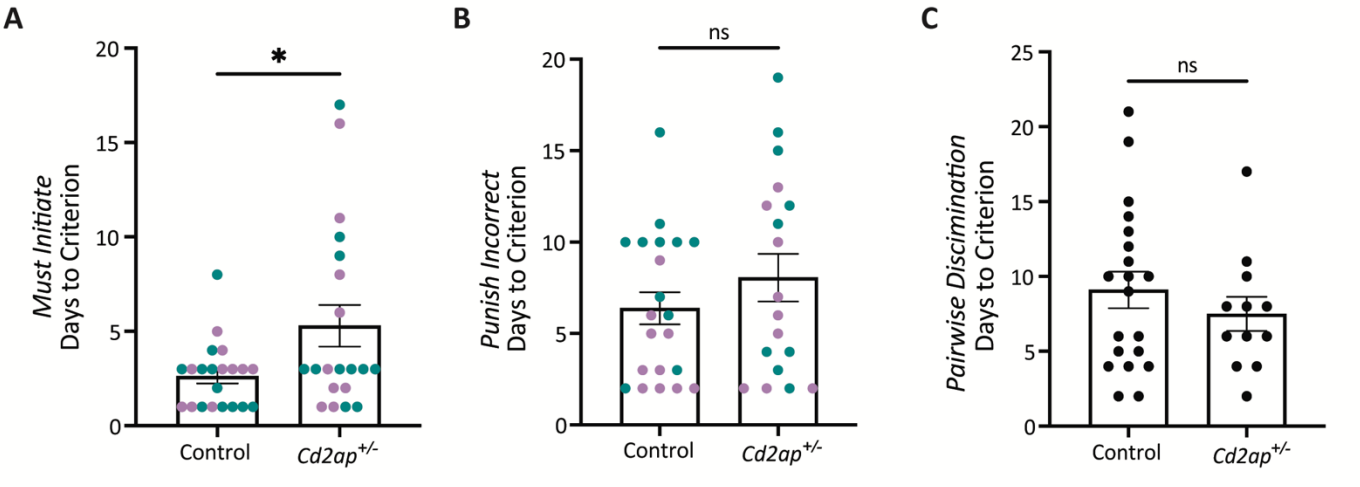

D

	No. mice that entered the module		No. mice that satisfied module criterion	
Module	Control	*Cd2ap+/-*	Control	*Cd2ap+/-*
Must Touch	22	21	21	20
Must Initiate	21	20	21	20
Punish Incorrect	21	20	21	18
Pairwise Discrimination	21	18	20	12

Supplemental Figure 10. Additional touchscreen testing of heterozygous *Cd2ap*$^{+/-}$ mice.

Statistical analysis was based on t-tests. All error bars indicate mean ± SEM. *, $P < 0.05$

(A) Young *Cd2ap*$^{+/-}$ mice show increased time for learning in the "must initiate" module. N = 21 (with 10 female and 11 male) wildtype controls and 20 (with 9 F and 11 M) *Cd2ap*$^{+/-}$ mice.

(B) Young *Cd2ap*$^{+/-}$ mice show no difference in the time for learning in the "punish incorrect" module. N = 21 (with 10 F and 11 M) wildtype control and 18 (with 9 F and 9 M) *Cd2ap*$^{+/-}$ mice.

(C) *Cd2ap*$^{+/-}$ mice successfully learning the visual discrimination task showed no difference in the number of days needed to reach criterion. N = 20 (with 9 F and 11 M) wildtype control and 12 (with 6 F and 6 M) *Cd2ap*$^{+/-}$ mice.

(D) Table listing the number of mice of each genotype that entered each touchscreen assay module and the number that pass the criterion for each module (criteria listed in main Fig. 6B). In each module, animals that fail to satisfy the criterion for that module drop out entirely and are not carried forward to the subsequent module, culminating in the pairwise discrimination test.

The color of individual data points in **(A)** and **(B)** indicates the sex of each animal, with teal indicating male mice and lavender indicating female mice.

Supplemental Figure 11.

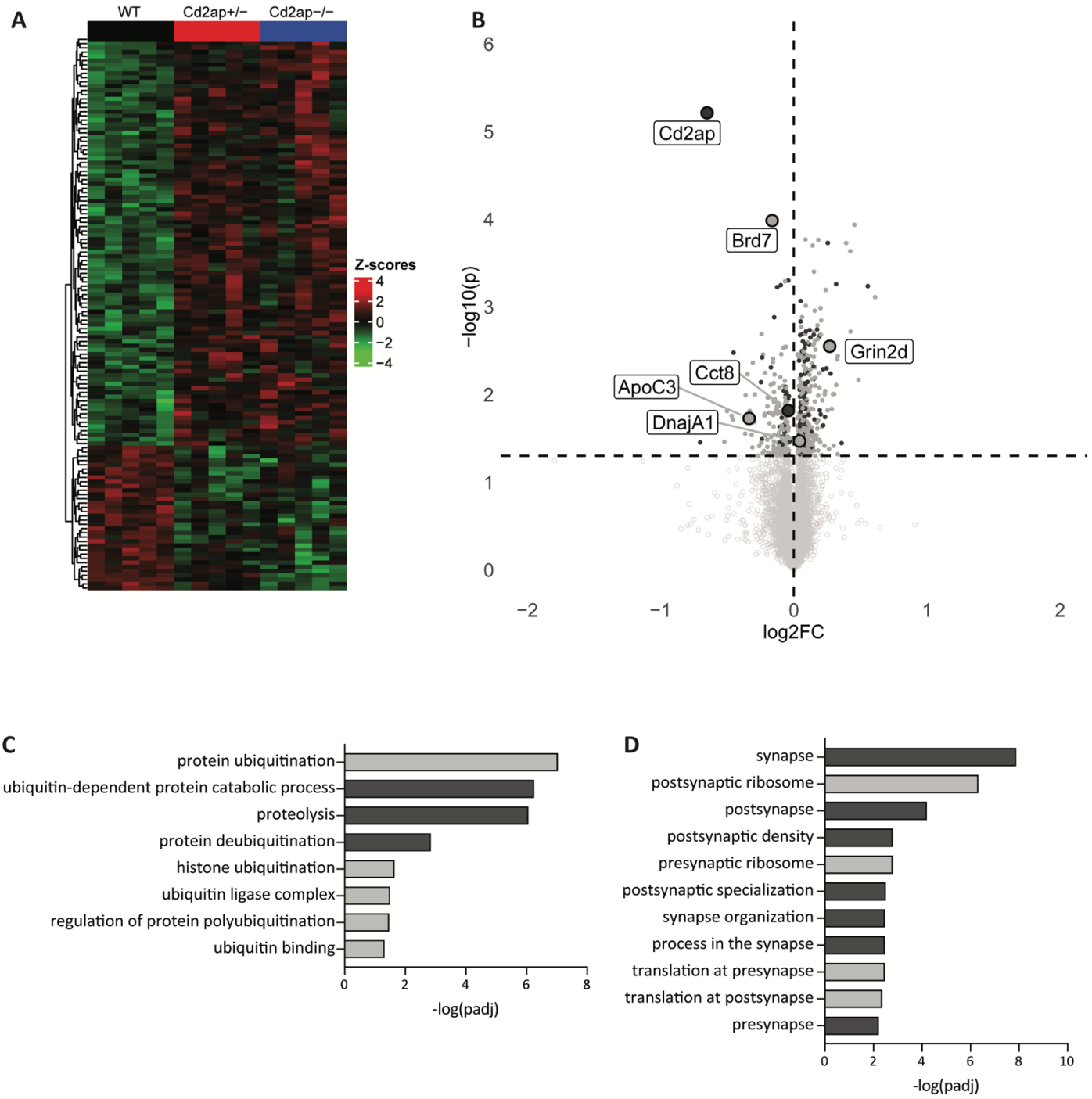

Supplemental Figure 11. Additional analysis of hippocampal proteomics from *Cd2ap*$^{-/-}$ and *Cd2ap*$^{+/-}$ mice.

(A) Heatmap showing mean-centered values (z-scores) for 130 shared differentially expressed proteins in *Cd2ap*$^{-/-}$ and *Cd2ap*$^{+/-}$. Rows were clustered using hierarchical clustering (ComplexHeatmap v.2.18.0).

(B) Volcano plot showing 508 differentially expressed proteins ($P < 0.05$) from comparisons of *Cd2ap*$^{+/-}$ heterozygotes with wildtype controls. Dark shading indicates proteins that also differentially expressed in *Cd2ap*$^{-/-}$ homozygotes.

(C-D) Selected, gene ontology term enrichment results related to proteasome and synaptic pathways, based on differential expression analysis of *Cd2ap*$^{-/-}$ hippocampi. Dark-shaded bars highlight pathways that were consistently enriched in *Cd2ap*$^{+/-}$ heterozygous mice. Statistical analysis used Fisher's exact test, FDR < 0.05.

Supplemental Figure 12.

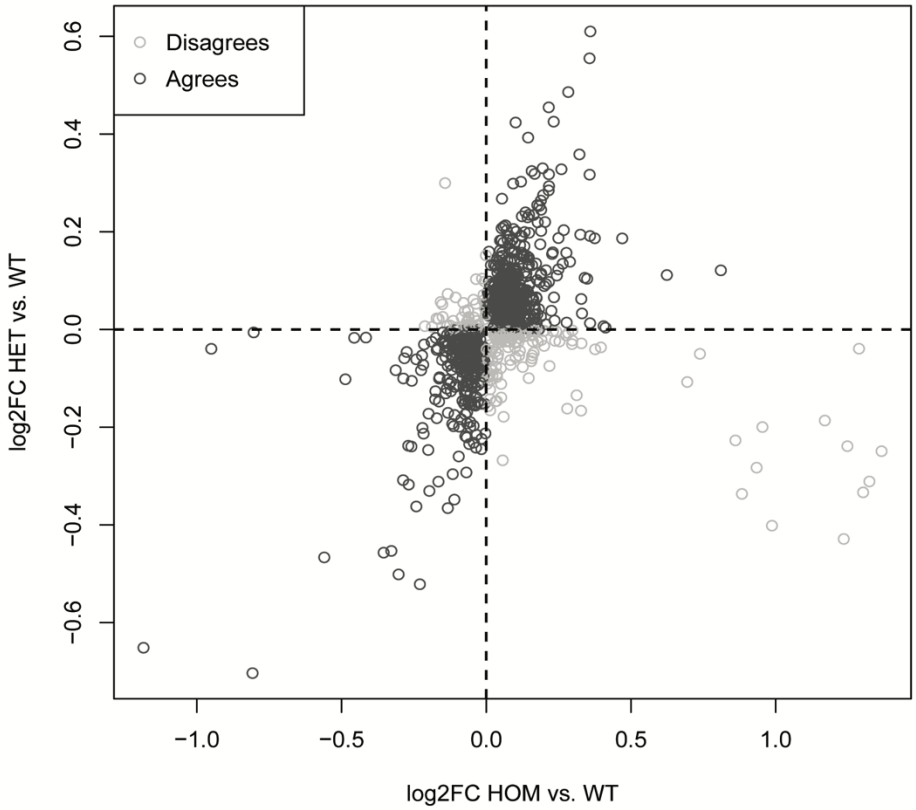

Supplemental Figure 12. Analysis of agreement of protein dysregulation directionality between *Cd2ap*$^{-/-}$ and *Cd2ap*$^{+/-}$.

1,207 proteins characterized as DEPs in *Cd2ap*$^{-/-}$ and/or *Cd2ap*$^{+/-}$ were plotted. Dark gray: Proteins that agree in directionality of change; Light gray: Proteins that disagree in directionality of change.

Supplemental Figure 13.

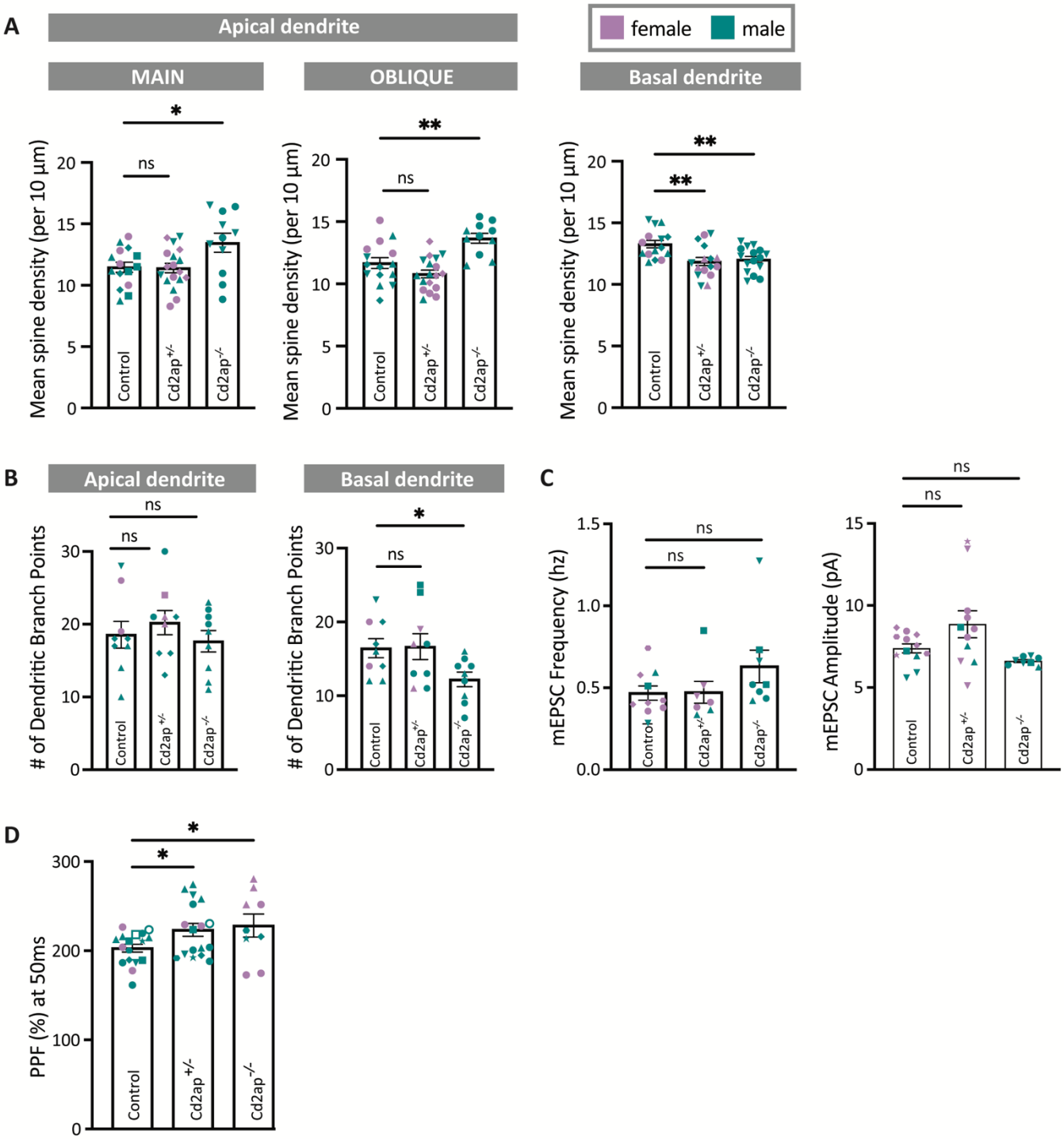

Supplemental Figure 13. Sex and animal of origin distribution of analyzed cells and slices from Figures 3 and 4.

(A) *Cd2ap*$^{-/-}$ mice have increased spine density on both main and oblique apical dendrites. Arrowheads indicate representative spines. By contrast, basal dendrites show decreased spine density in both *Cd2ap*$^{-/-}$ and *Cd2ap*$^{+/-}$ mice. Statistical analysis was based on t-tests. For apical dendrites, samples sizes (number of cells quantified) were WT = 15 (4 female and 11 male); *Cd2ap*$^{+/-}$ = 18 (10F and 8M); and *Cd2ap*$^{-/-}$ = 11 (11M). For basal dendrites samples sizes were WT = 15 (4F and 11M); *Cd2ap*$^{+/-}$ = 16 (8F and 8M); and *Cd2ap*$^{-/-}$ = 16 (16M). For both apical and basal dendrites, samples sizes (number of mice) were WT = 4 (1F and 3M); *Cd2ap*$^{+/-}$ = 4 (2F and 2M); and *Cd2ap*$^{-/-}$ = 2 (2M). * = $P < 0.05$; ** = $P < 0.01$. All error bars denote mean ± SEM.

(B) Dendritic branching of basal but not apical ($P > 0.05$), dendrites is decreased in *Cd2ap*$^{-/-}$ mice, based on t-tests. No change was observed in *Cd2ap*$^{+/-}$ heterozygotes for either apical or basal dendrites ($P > 0.05$). Samples sizes were N = 9 cells for each group. Sex distribution of the cells' animals of origin was as follows: WT had 2F and 7M cells; *Cd2ap*$^{+/-}$ had 3F and 6M cells; and *Cd2ap*$^{-/-}$ had all M cells. Samples sizes (number of mice) were WT = 4 (1F and 3M); *Cd2ap*$^{+/-}$ = 4 (2F and 2M); and *Cd2ap*$^{-/-}$ = 2 (2M). * = $P < 0.05$. All error bars denote mean ± SEM.

(C) mEPSC frequency and amplitude are not significantly changed in *Cd2ap* homozygous or heterozygous animals ($P > 0.05$; ns, non-significant), when compared with wildtype controls (WT). Statistical analysis was performed using one-way ANOVA with Dunnett's post-hoc test. For analysis of mEPSC frequency, sample sizes (N cells recorded) were as follows: WT = 10 (7 female and 3 male); *Cd2ap*$^{+/-}$ = 7 (4F and 3M); and *Cd2ap*$^{-/-}$ = 8 (8M). For analysis of mEPSC amplitude, sample sizes were as follows: WT = 12 (8F and 4M); *Cd2ap*$^{+/-}$ = 11 (8F and 3M); and *Cd2ap*$^{-/-}$ = 8 (8M). Samples sizes (number of mice) were WT = 7 (4F and 3M); *Cd2ap*$^{+/-}$ = 5 (3F and 2M); and *Cd2ap*$^{-/-}$ = 4 (4M). All error bars denote mean ± SEM.

(D) Paired pulse facilitation (PPF) is increased in both *Cd2ap* homozygous and heterozygous animals, when compared with WT controls for the 50ms inter-stimulus interval trial, based on t-tests with sample sizes (slices recorded): WT = 17 (3F and 14M); *Cd2ap*$^{+/-}$ = 17 (2F and 15M); and *Cd2ap*$^{-/-}$ = 9 (6F and 3M). Samples sizes (number of mice) were WT = 10 (1F and 9M); *Cd2ap*$^{+/-}$ = 9 (1F and 8M); and *Cd2ap*$^{-/-}$ = 5 (2F and 3M). *, $P < 0.05$. All error bars denote mean ± SEM.

For all three genotypes in **(A), (B)**, **(C)**, and **(D)** datapoints (cells or slices) from different animals within a gender are represented by different shapes. Cells that originated from male mice are teal and cells that originated from female mice are lavender.